Vortex nucleation as a case study of symmetry breaking in quantum systems

D. Dagnino[1], N. Barberán[1], M. Lewenstein[2,3], and J. Dalibard[4]
(1) Dept. ECM, Facultat de Física, Universitat de Barcelona, E-08028 Barcelona, Spain
(2) ICFO - Institut de Ciències Fotòniques, Parc Mediterani de la Tecnologia 08860 Barcelona, Spain
(3) ICREA– Institució Catalana de Recerca i Estudis Avançats, E-08010, Barcelona, Spain
(4) Laboratoire Kastler Brossel, CNRS, UPMC, Ecole Normale Supérieure, 24 rue Lhomond, 75005 Paris, France
(Dated: December 21, 2009)

Mean-field methods are a very powerful tool for investigating weakly interacting many-body systems in many branches of physics. In particular, they describe with excellent accuracy trapped Bose-Einstein condensates. A generic, but difficult question concerns the relation between the symmetry properties of the true many-body state and its mean-field approximation. Here, we address this question by considering, theoretically, vortex nucleation in a rotating Bose-Einstein condensate. A slow sweep of the rotation frequency changes the state of the system from being at rest to the one containing one vortex. Within the mean-field framework, the jump in symmetry occurs through a turbulent phase around a certain critical frequency. The exact many-body ground state at the critical frequency exhibits strong correlations and entanglement. We believe that this constitutes a paradigm example of symmetry breaking in - or change of the order parameter of - quantum many-body systems in the course of adiabatic evolution.

PACS numbers: 03.75.Hh, 03.75.Kk, 67.40.Vs

In classical physics, examples of the usefulness of mean-field theory go back to the "molecular field theory" of magnetism [1]. In the classical world, symmetry changes (or breaking) are driven by thermal fluctuations, and in the standard Landau-Ginsburg scenario are associated with increase of classical correlations. In quantum physics, the paradigm example of applicability of the mean field concerns a weakly interacting quantum Bose gas and Bose-Einstein condensation [2]. The mean-field description of the gas assumes that its ground state Ψ is approximated by a product state $\Psi(\vec{r}_1,\ldots,\vec{r}_N) = \psi(\vec{r}_1)\ldots\psi(\vec{r}_N)$, of essencially uncorrelated particles forming a superfluid Bose-Einstein condensate with order parameter ψ.

Of particular interest for quantum gases are quantum phase transitions and symmetry changes/breaking driven by quantum fluctuations. A celebrated example is the superfluid to Mott-insulator transition of bosons in an optical lattice [3]. Another example yet to be explored experimentally is the case of a fast rotating gas, when the number of vortices is similar to the number of particles, or equivalently angular momentum $L \sim N^2$ [4]. The ground state of the system is then a strongly correlated quantum liquid such as the Laughlin state, analogous to those emerging in quantum Hall physics [5]. Here, we consider another situation, dealing with the case of a relatively slowly rotating gas at the threshold of the nucleation of the first vortex. We show that owing to the symmetries of the system, the many-body state at nucleation is strongly correlated and characterize its properties.

The symmetry change/breaking that results from vortex nucleation has drawn a lot of attention since the discovery of superfluids [6]. For quantum gases, atoms are usually confined in an isotropic harmonic trap and experience an extra quadratic potential rotating at angular frequency Ω (for a review see ref.7). From a theoretical point of view, the vortex nucleation can be tackled by several techniques, ranging from a mean-field approach based on the Gross-Pitaevskii equation [8, 9, 10] to the investigation of the many-body energy eigenstates [11, 12, 13, 14, 15, 16, 17]. Within the mean field framework, standard textbooks [2] associate vortex nucleation with thermodynamic instability. Above a critical rotation frequency Ω_c, the odd solution ψ of the Gross-Pitaevskii equation with a single vortex [18, 19] has a lower energy than the even solution corresponding to the Bose-Einstein condensate at rest [20]. Here, we go beyond the mean-field approach and study the exact quantum dynamics of a mesoscopic sample of atoms, in the presence of the stirring potential. Our main result is that for a rotation frequency close to Ω_c, the mean-field description is invalid. The system enters a strongly correlated and entangled state, well described by an effective two-mode model. We compare our results with those obtained from a mean-field description and show that the latter exhibits dynamical instability and hysteresis. As we explicitly include here an anisotropic stirring potential, the present mechanism concerns a discrete parity symmetry breaking. Therefore, it differs from the case of the vortex nucleation in axially symmetric traps: in the latter case, breaking of the continuous rotational symmetry involves a gapless Nambu-Goldstone mode [21], whereas here we deal with a gapped system.

Model. We consider a mesoscopic sample of N bosonic atoms of mass M placed in an axially symmetric harmonic potential V_0, with frequency $\omega_\perp$ in the xy plane and ω_z along the z axis. Here, $\hbar\omega_z$ is large compared with the interaction energy so that the dynamics along z is frozen and the gas is effectively two-dimensional (2D) at sufficiently low temperature. The gas is set in rotation using an anisotropic quadratic potential V in the xy plane, rotating at angular frequency Ω around the z axis. In the rotating frame, this stirring potential reads $V(x,y) = 2AM\omega_\perp^2(x^2-y^2)$, where the coefficient A ($\ll 1$) measures the strength of the anisotropy.

For $A \ll 1$ and $\Omega \sim \omega_\perp$, the single-particle energy levels in the rotating frame are grouped in Landau levels, separated by $\hbar(\omega_\perp+\Omega)$ (refs.7,22). We assume that $\hbar(\omega_\perp+\Omega)$ is

large compared with the interaction energy, so that the atomic dynamics is restricted to the lowest Landau level (LLL). For $A = 0$, a basis of the LLL single-particle states is the set $\varphi_m(x,y) \propto (x+iy)^m e^{-(x^2+y^2)/2\lambda_\perp^2}$, where $m \geq 0$ is an integer and $\lambda_\perp = \sqrt{\hbar/M\omega_\perp}$. Each φ_m is an eigenstate of the z-component of the single-particle angular momentum (eigenvalue $m\hbar$) and of the single-particle Hamiltonian without anisotropy (eigenvalue $\hbar[\omega_\perp + m(\omega_\perp - \Omega)]$). Within the LLL, we model the atomic interactions by a 2D contact potential $U(\vec{r}) = (\hbar^2 g/M)\,\delta(\vec{r})$ where $g = \sqrt{8\pi}a/\lambda_z$ is dimensionless, a is the 3D scattering length and $\lambda_z = \sqrt{\hbar/M\omega_z}$. We choose $\lambda_\perp$, $\hbar\omega_\perp$ and $\omega_\perp$ as units of length, energy and frequency.

Energy spectrum. We first recall some important properties of the N-particle system in absence of anisotropy ($A = 0$). In this case, the total angular momentum operator $\hat{L}$ commutes with the Hamiltonian $\hat{H}$ so that one can look for the eigenstates of $\hat{H}$ within subspaces $\mathcal{E}_L$ of fixed L. The lowest-energy state in each $\mathcal{E}_L$ for $2 \leq L \leq N$ is [12, 13, 14]:

$$\Phi_L(\vec{r}_1,\ldots,\vec{r}_N) \propto \sum_{1\leq i_1 \ldots \leq i_L} (u_{i_1} - u_c)\ldots(u_{i_L} - u_c)\,\Phi_0$$

where $u_j = x_j + iy_j$, $u_c = \sum_j u_j/N$ and

$$\Phi_0(\vec{r}_1,\ldots,\vec{r}_N) \propto e^{-\sum_j r_j^2/2}\,.$$

The energy of the state Φ_L is $N + (1-\Omega)L + gN(2N - L - 2)/(8\pi)$. At $\Omega_1 = 1 - gN/(8\pi)$, all Φ_L states for $L = 0$ and $2 \leq L \leq N$ are degenerate. The angular momentum of the ground state $L_{\rm GS}(\Omega)$ shows sharp steps at critical values $\Omega_i, i = 1, 2, ..$ (ref.23). Below Ω_1, the ground state is the zero angular momentum state Φ_0. At Ω_1, $L_{\rm GS}$ jumps from 0 to N. Above Ω_1 the ground-state angular momentum has a plateau $L = N$ up to Ω_2, where a second jump takes place. From this value, a sequence of jumps and plateaux emerges up to the last possible L value, $L = N(N-1)$, corresponding to the Laughlin state. In the following, we focus on the vicinity of the first jump $\Omega \sim \Omega_1$, where the first vortex is nucleated.

We now turn to the case where the rotating anisotropy is present. The many-body energy spectrum is calculated numerically by diagonalization of the Hamiltonian (see the Methods section). We show it in Fig.1 for both zero anisotropy and for $A = 0.03$, using $N = 6$ for illustration. The interaction coupling $g = 1$ so that $\Omega_1 = 0.761$. For $A \neq 0$ the ground state does not show any degeneracy around Ω_1, contrary to the case $A = 0$. In Fig.2, we compare $L_{\rm GS}(\Omega)$ for $A = 0$ and $A = 0.03$. For $A \neq 0$ $L_{\rm GS}$ evolves smoothly from 0 to N around Ω_1.

Failure of the mean-field approach for $\Omega \sim \Omega_1$. We now explain why a mean-field description must fail at $\Omega \simeq \Omega_1$. We notice that the total Hamiltonian is parity invariant. Consequently, one can look for an eigenbasis of the N-body Hilbert space composed of either even or odd states. From the ground state of the Hamiltonian, we can extract the single-particle density matrix (SPDM) $n^{(1)}(\vec{r},\vec{r}')$ (see the Methods section),

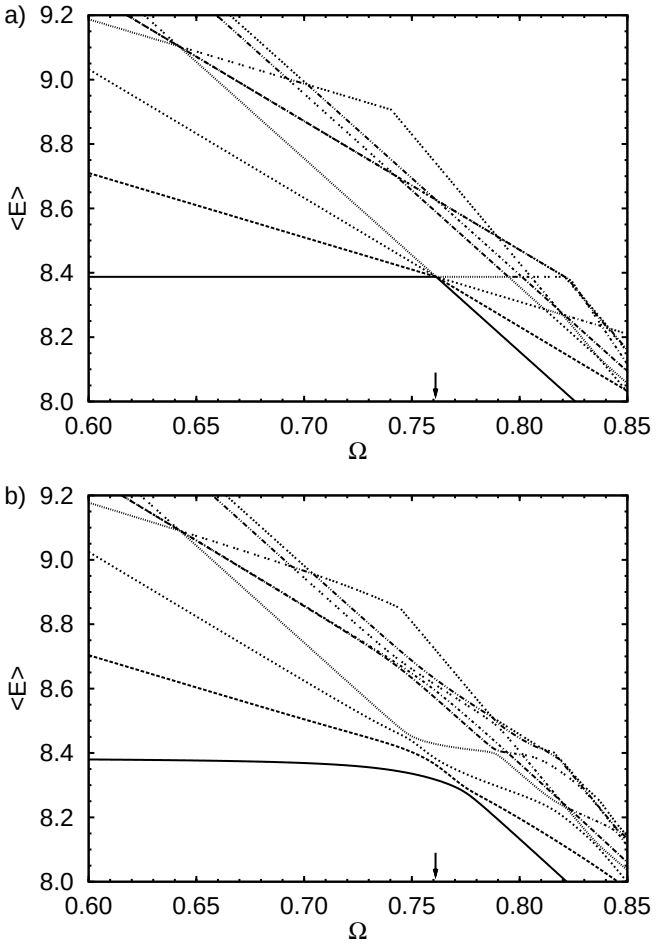

FIG. 1: **Energy spectrum as a function of** Ω**. a**, Anisotropy parameter $A = 0$. **b**, $A = 0.03$. In both cases, $N = 6$ and $g = 1$. For $A = 0$, the ground state is multiply degenerate at the rotation frequency $\Omega_1 = 1 - gN/(8\pi)$, which corresponds to the nucleation frequency of the first vortex. A non-zero anisotropy parameter lifts the degeneracy of the groun state. Here, we plot only the first nine energy eigenvalues from the subspace formed with even values of the total angular momentum, which are the only relevant ones for the problem addressed in this article. The arrows mark the value of Ω_1.

which is also parity invariant. Hence, the single-particle orbitals ψ_k, which are eigenstates of $n^{(1)}$ with eigenvalues n_k ($\sum_k n_k = N$), can also be chosen with even or odd parity. Suppose that we vary Ω from an initial value Ω_i ($\Omega_i < \Omega_1$) to a final value Ω_f ($\Omega_1 < \Omega_f < \Omega_2$), choosing $\Omega_{i,f}$ in a region where the mean-field description is valid, that is, when the largest eigenvalue n_1 is close to N. For $\Omega_i < \Omega_1$ the most (second most) populated state ψ_1 (ψ_2) has no (has a) vortex in its central region and is even (odd). Choosing $\Omega_i = 0.7$, we plot the phase profiles of $\psi_{1,2}$ in the first row of Fig.3 for $N = 6$ atoms, $g = 1$ and $A = 0.03$. On the other hand, at Ω_f the ground state has a single well-centered vortex and ψ_1 and ψ_2 are odd and even, respectively (see last row of Fig.3 for $\Omega = 0.8$). Hence, the parity of ψ_1 must change at some intermediate Ω_c, which is close (for small A) to the vortex nucleation frequency Ω_1 in absence of anisotropy. By conti-

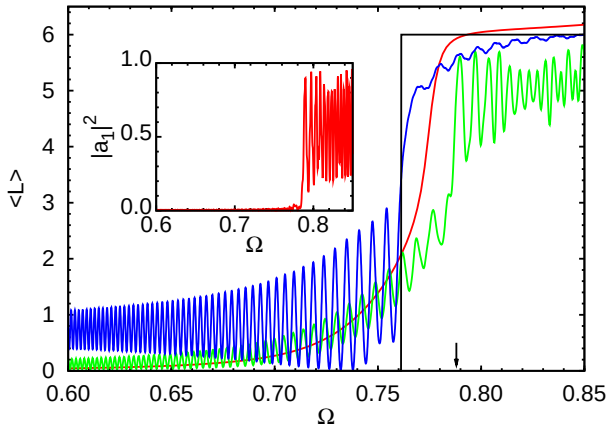

FIG. 2: **Variation of the angular momentum with rotation frequency** Ω. The black and red lines show, for an anisotropy $A = 0$ and $A = 0.03$ respectively, the angular momentum of the ground state for a system of $N = 6$ particles and an interaction strength $g = 1$. The green line is the average angular momentum predicted by the mean-field treatment when Ω is linearly ramped from 0 to 0.85 with a slope $\dot{\Omega} = 10^{-4}$. The initial state at $\Omega = 0$ is given by a slight perturbation of the coefficients $a_0 = 1$, $a_1 = a_2 = 0$. It presents a dynamical instability of the zero-vortex mean-field solution for $\Omega = 0.788$ (marked by an arrow). Inset: The evolution of $|a_1|^2$, which explicitly shows the instability. The blue curve of the main figure is the backward evolution corresponding to an initial state at $\Omega = 0.85$ close to the stationary mean-field solution $a_0 = a_2 = 0$ and $a_1 = 1$. This solution ceases to exist for $\Omega < 0.764$, causing the large oscillations in the evolution of the angular momentum.

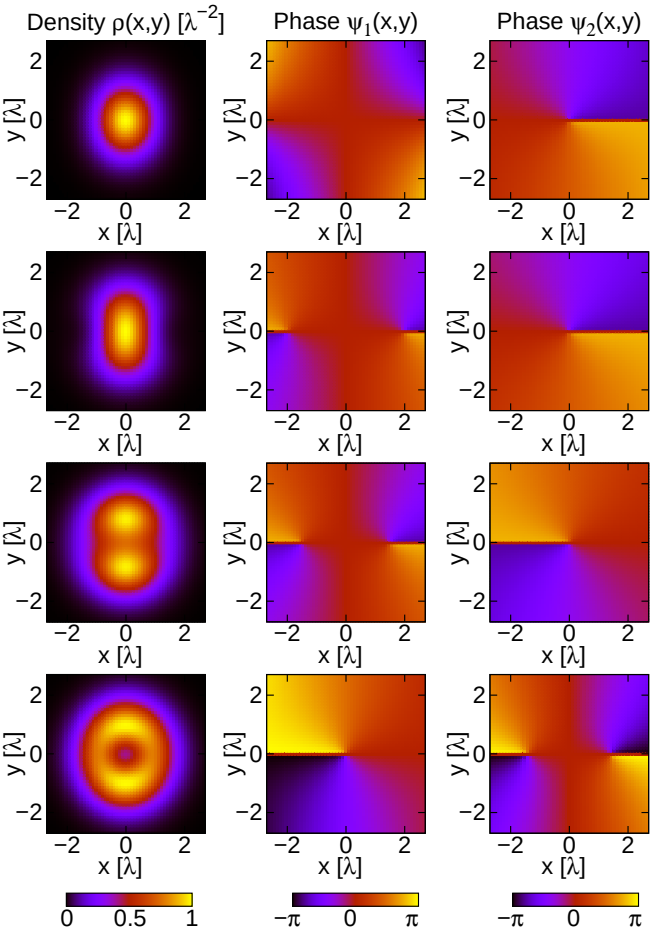

FIG. 3: **Density of the ground state and phase maps of ψ_1 and ψ_2.** Four different values of Ω for $N = 6$, $A = 0.03$ and $g = 1$ are considered. First row: $\Omega = 0.7$, $n_1 = 5.85$, $n_2 = 0.12$. Second row: $\Omega = 0.760$, $n_1 = 5.01$, $n_2 = 0.60$. Third row: $\Omega = \Omega_c = 0.776$ $n_1 = n_2 = 2.88$. Fourth row: $\Omega = 0.8$ with $n_1 = 4.24$, $n_2 = 1.07$. The first column is the contour plot of the total density, and the second and third columns show the local phase maps of ψ_1 and ψ_2 respectively. Vortices are localized at the singularities of the phase maps, surrounded by diffuse change of the phase. This figure shows that the nucleation of the first centered vortex in a rotating condensate by a slow frequency sweep does not occur through a smooth entrance of the vortex. The system passes through a correlated, non-mean-field state where two single-particle states have equal weight. At this point, ψ_1 changes from being a coherent superposition of φ_0 and φ_2 (two off-centered vortices) to the single φ_1 state, which corresponds to a well-centered single vortex. Simultaneously, ψ_2 experiences the inverse change.

nuity, the two most populated eigenstates ψ_1 and ψ_2 of $n^{(1)}$ must have equal populations, heralding a failure of the mean-field at Ω_c.

We show in Fig.4 the variation of n_1/N and n_2/N as a function of Ω, for $N = 12$, $g = 0.5$ and $A = 0.03$. These two populations are equal for $\Omega_c = 0.775$. We see that $n_1 + n_2 \simeq N$ over the whole range of frequencies of this figure, indicating that most of the population of the SPDM is concentrated in the first two modes ψ_1 and ψ_2. We checked up to $N = 20$ that this concentration increases with N. Another relevant fact is that only the first three LLL single-particle states ($m = 0, 1, 2$) have a significant weight in the expansion of ψ_1 and ψ_2. More specifically, below Ω_c ψ_1 is approximately a coherent superposition of φ_0 and φ_2, corresponding to two off-centered vortices (even parity), whereas ψ_2 is very close to a well-centered single-vortex state φ_1 (odd parity). Above Ω_c, ψ_1 and ψ_2 abruptly exchange their form (see Fig.3).

The failure of the mean-field description around Ω_c may occur in two ways. A first possibility is that for $\Omega = \Omega_c$, the many-body ground level itself has a two-fold degeneracy with two eigenstates of opposite parity. This scenario corresponds to a first-order transition. It occurs when N is odd, because the graund state evolves from $\sim \psi_1^{\otimes N}$ with ψ_1 even to $\sim \psi_1^{\otimes N}$ with ψ_1 odd. The second possibility is that the many-body graund state $|\Psi_0\rangle$ remains non-degenerate, as this is the case in Fig.1b. In this case, $|\Psi_0\rangle$ is even over the whole range $[\Omega_i, \Omega_f]$. This occurs for even N and will be of interest for the rest of the article.

Quantum correlations for $\Omega \sim \Omega_c$. We have carried out a detailed study of the ground state $|\Psi_0\rangle$ around the critical frequency Ω_c, where the two largest eigenvalues of the SPDM are equal ($n_1 = n_2$). At criticality, the system is very well described by a two-mode approximation implied by Fig.4a. The two largest eigenvalues of the SPDM are much larger than

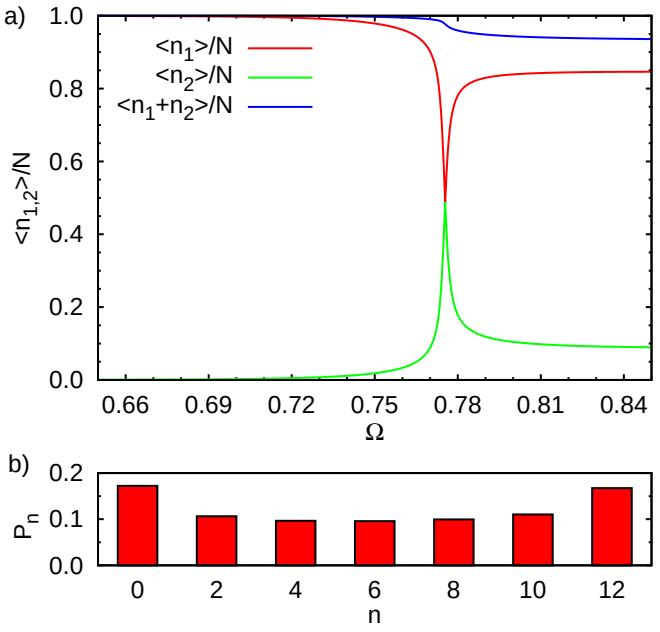

FIG. 4: **Structure of the ground state. a**, Variation of the relative populations n_1/N and n_2/N of the two most occupied states ψ_1 and ψ_2 of the SPDM. When Ω is sufficiently different from Ω_c, $n_1 \simeq N$, the system is well described by a single mode and the mean-field description is valid. Conversely, for $\Omega \simeq \Omega_c$, the two populations are comparable, corresponding to the case where a two-mode approximation is valid even in the entangled region. **b**, Analysis of the state of the system at the critical point where $n_1 = n_2$, in terms of the square of the scalar products $P_n = | \langle n : \psi_1 \ ; \ N-n : \psi_2 | \Psi_0 \rangle |^2$. We obtain $| \langle E \mid \Psi_0 \rangle | = 0.92$ (see equation (1)). Both panels are plotted for $N = 12$, $g = 0.5$ and $A = 0.03$.

all of the others, so that $n_1 = n_2 \simeq N/2$. For example, for $N = 12$, $g = 0.5$ and $A = 0.03$, we obtain $n_1 = n_2 = 0.49\,N$ at $\Omega_c = 0.776$. The ground state is strongly correlated and is well described (for even N) by

$$|E\rangle = [|N,0\rangle + |N-2,2\rangle + ... + |0,N\rangle]/\sqrt{N/2+1}, \quad (1)$$

where $|n,m\rangle$ is the state with n (respectively m) atoms in ψ_1 (respectively ψ_2). Amazingly, the form of the ground state at Ω_c is practically independent of A, as long as $A \ll 1$. For a quantitative comparison of the exact ground state with the state (1), we show in Fig.4b the squared scalar products $\langle n, N-n|\Psi_0\rangle$ in the case $N = 12$. They are all zero for odd values of n (as expected from the parity of $|\Psi_0\rangle$) and approximately constant for even values of n. We compared also our ground state at Ω_c with other celebrated correlated states, such as "Schrödinger cat" states $(|N,0\rangle + |0,N\rangle)/\sqrt{2}$, or "twin" states $|N/2, N/2\rangle$, and found much smaller overlaps. Although there are various ways of defining entanglement for identical particles (for a review see [24]), according to Zanardi's concept of mode entanglement (ref.24), the state (1) is maximally entangled. This is clearly seen by tracing the state (1) over one of the two modes and observing that the von Neumann entropy of the reduced density matrix reaches the maximal value $S \sim \log(N)$.

At this point we mention related work on rotating ring lattices and Josephson junctions [26]. There, strongly correlated states are predicted at critical rotation, but the mechanism of their generation, as well as their nature are fundamentally different. The starting situation of these discretized models is that there are two degenerated single-particle states. Interactions lift the degeneracy in the many-body system and favor the "cat" states. In our case, the ground state for $A = 0$ is macroscopically degenerated in the presence of interactions. The degeneracy is lifted here by the anisotropy, leading to another kind of strongly correlated ground state.

Vortex nucleation with adiabatic passage. We now study the real-time dynamics of the system using the time-dependent Schrödinger equation. A quasi-adiabatic evolution that brings the system from the zero-vortex to the one-vortex state, is realized by sweeping Ω: $\Omega(t) = \Omega_{\rm i} + \gamma t$ from the initial frequency Ω_i chosen well below Ω_c (typically $\Omega_i = 0.65$) to the final frequency $\Omega_{\rm f}$, well above Ω_c (typically $\Omega_f = 0.85$). This evolution produces as an intermediate step the strongly correlated state (1). The key parameter for the success of this quasi-adiabatic evolution is the energy gap Δ between the ground state and the first excited state of the system.

We have carried out a study of this gap for various N, keeping the product Ng constant so that Ω_1 also remains constant. We found that for small A values (below 0.1), the gap is roughly constant over the range $10 \leq N \leq 20$, and equal to $\simeq 0.5\ A$. Knowing the gap, we estimate the largest possible γ compatible with adiabatic evolution following ref. 27 and find $\gamma_{\rm max} = \xi\ \Delta^2/N$, where $\xi \ll 1$ (see the Methods section). This criterion agrees well with our results. Defining as successful an adiabatic evolution that leads to an overlap larger than 0.98 between the final state and the ground state at Ω_f, we find $\xi \simeq 0.1$ for $10 \leq N \leq 20$. Such a quasi-adiabatic evolution anables us to attain the correlated state (1) with comparable overlap. For practical implementations, the atoms can be confined in a relatively tight trap at the nodes of an optical lattice with $\omega_\perp/2\pi$ in the 10 kHz range. For an anisotropy $A = 0.1$ and $N = 10$ atoms, the sweep time has to be of the order of one second to ensure adiabaticity.

A natural question is the generalisation of the present scheme to large N. Assuming that the gap protecting the ground state remains constant, the mechanism will in principle survive. However, we have neglected here any parity-breaking perturbation in the Hamiltonian. Such a term would couple the subspaces corresponding to even and odd L values. As shown in ref. 17, the lowest energies of these two subspaces are exponentially close when N increases, wich affects the robustness of the ground state. This coupling thus constitutes an important decoherence mechanism for large N, whereas our scheme remains valid for N not exceeding a few tens.

Mean field approach. As our results point out that strongly correlated states may be reached in the course of the time evolution, it is interesting to see what the predictions of usual mean-field theory are. To this aim, we ex-

pand the condensate wavefunction $f(\vec{r},t)$ into the relevant single particle LLL orbitals $\varphi_m(\vec{r})$ with angular momentum $m = 0, 1, 2$, $f(\vec{r},t) = \sum_{m=0}^{2} a_m(t)\varphi_m(\vec{r})$. Using the dynamical variational principle [28], we derive Lagrange equations for the complex amplitudes $a_m(t)$ (see the Methods section), and look for the stationary solutions of the form $a_m(t) = \exp(-i\mu t)a_m(0)$ and their stability. Finally, we evolve the mean-field equations and compare the results with the full quantum treatment.

We choose $gN = 6$ and $A = 0.03$. Among the several possible stationary solutions, two of them are relevant. The first one f_a corresponds to the "no vortex" situation with a small admixture of "two-vortex" orbital, that is, $|a_0| \simeq 1, |a_2| \ll 1$ and $a_1 = 0$. This solution is the ground state for $\Omega < \tilde{\Omega} = 0.773$. The second relevant solution f_b contains a non-zero contribution of the one-vortex state ($a_1 \neq 0$) and it is the ground state for $\Omega > \tilde{\Omega}$. Thus, $\tilde{\Omega}$ marks the critical value of Ω for the thermodynamical stability of a centred vortex, and the "first-order transition" within the mean-field approach.

In the frequency range $0.764 < \Omega < 0.788$, both solutions exist and are stable, leading to a bistable and hysteresis behaviour. For $\Omega > 0.788$, f_a becomes dynamically unstable ($|a_1|$ grows exponentially in time, starting from noise, see inset in Fig. 2). For $\Omega < 0.764$, f_b does not exist. The numerical study confirms this hysteresis behaviour, as shown in Fig. 2. The green line shows the angular momentum when Ω is ramped linearly in time from $\Omega_i = 0$ to $\Omega_f = 0.85$, with the rate $\dot{\Omega} = 10^{-4}$. A turbulent behaviour occurs once $\Omega(t)$ reaches the edge of the stability domain of f_a. The blue line shows the reverse evolution in which Ω varies from Ω_f to Ω_i at the same rate. Evidently, the adiabatic character of the dynamics cannot be maintained, in contrast to the result of the exact many-body treatment.

Summary We conjecture that the scenario presented above is generic for the following situations: (1) it concerns quantum mechanical systems in which the ground state undergoes symmetry change/breaking as some parameter of the system λ crosses a critical value λ_c; (2) far from λ_c, the systems are well described by the mean-field theory with order parameters reflecting the change of symmetry; (3) in the dynamical mean-field description, the system exhibits dynamical instability and breakdown of adiabaticity.

In such situations we expect the appearance of strongly correlated states. The SPDM shows typically a few relevant single-particle modes that are involved in the symmetry change. They can be guessed by analyzing the results of the dynamical mean-field approach. For instance, if this approach exhibits standard signatures of bistability, we can expect two relevant modes as in the case study presented here. Similar insight can be gained from analysis of small Gaussian fluctuations around the mean-field solutions, that is, Bogoliubov-de Gennes equations [29]. Reduction of the full theory to the quantum modes provides then a very good approximation. Alternatively, it can be viewed as re-quantization of the mean-field theory reduced to the relevant single-particle orbitals [17]. The strongly correlated states appearing in such a situation exhibit strong entanglement and this property can be detected in experiments with moderate N.

Methods

Diagonalization of the Hamiltonian. In the frame rotating at angular frequency Ω, the Hamiltonian of the system is $H = H_0 + U$, where H_0 is the sum of one-body Hamiltonians $H_0 = \sum_{j=1}^{N} H_{0,j}$ and U is the two-body interaction potential, characterized by the 3D scattering length a. Each one-body Hamiltonian is the sum of kinetic, potential and rotation energy:

$$\begin{aligned} H_{0,j} &= \frac{p_j^2 + p_{zj}^2}{2M} + \frac{M}{2}(\omega_\perp^2 r_j^2 + \omega_\parallel^2 z_j^2) \\ &- \Omega L_{z,j} + V_j \end{aligned}$$

where $V_j = 2AM\omega_\perp^2(x_j^2 - y_j^2)$ is the anisotropic potential that sets the gas in rotation. We assume that the interaction energy is much smaller than $\hbar\omega_z$ so that the z motion is frozen and the atoms occupy only the ground state $\exp(-z^2/(2\lambda_z^2))$ of this degree of freedom. The gas is supposed to be rotating sufficiently fast to have $\omega_\perp - \Omega \ll \omega_\perp + \Omega$, which guarantees that the various Landau levels are well separated from each other. The interaction energy is also assumed to be small compared to $\hbar(\omega_\perp + \Omega)$ so that the low temperature dynamics is restricted to the LLL.

In the absence of anisotropic potential $A = 0$, the eigenstates of the one-body Hamiltonian in the LLL are the functions $\varphi_m(x,y) \propto (x+iy)^m e^{-(x^2+y^2)/2\lambda_\perp^2}$, $m = 0, 1, 2, \ldots$. We introduce the creation $a_m^\dagger$ and annihilation a_m operators of an atom in state φ_m, and we write H in the second quantization

$$\hat{H} = \hbar\,\omega_\perp \hat{N} + \hbar\,(\omega_\perp - \Omega)\hat{L} + \hat{V} + \hat{U}\ ,$$

where $\hat{N} = \sum a_m^\dagger a_m$ and $\hat{L} = \sum m a_m^\dagger a_m$ are the particle number operator and the total z-component angular momentum operator, respectively. The expression of the rotating potential in the second quantization is

$$\begin{aligned} \hat{V} &= \frac{A}{2}\lambda_\perp^2 \sum_m \Big(\sqrt{m(m-1)}\; a_m^\dagger\, a_{m-2} \\ &+ \sqrt{(m+1)(m+2)}\; a_m^\dagger\, a_{m+2} \Big)\ . \end{aligned}$$

Finally the contact interaction potential reads

$$\hat{U} = \frac{1}{2} \sum_{m_1 m_2 m_3 m_4} U_{1234}\ \ a_{m_1}^\dagger a_{m_2}^\dagger a_{m_4}\, a_{m_3}\ ,$$

where the matrix elements are given by

$$\begin{aligned} U_{1234} &= \langle m_1\, m_2 \mid U \mid m_3\, m_4 \rangle \\ &= \frac{g}{\lambda_\perp^2 \pi}\ \frac{\delta_{m_1+m_2,m_3+m_4}}{\sqrt{m_1! m_2! m_3! m_4!}}\ \frac{(m_1+m_2)!}{2^{m_1+m_2+1}}\ . \end{aligned}$$

In the absence of anisotropy ($A = 0$), $\hat{H}$ and $\hat{L}$ commute and share a common basis. The first step in the diagonalization of the Hamiltonian is to determine a basis $|\Lambda_p\rangle$ ($p = 1, \ldots, n_L$) for each subspace of given total angular momentum L. The dimension n_L of each subspace corresponds to all of the possible configurations of N particles with angular momentum m_j that fulfil the condition $L = \sum_{j=1}^{N} m_j$. The matrix of the Hamiltonian in the LLL basis then consists of blocks of size $n_L \times n_L$, which we diagonalize using standard codes.

When $A \neq 0$, the anisotropic potential connects the various subspaces of given L. We then choose a maximum angular momentum $L_{\max}$ and write the matrix giving the restriction of the Hamiltonian to the subspace of states with $L \leq L_{\max}$. This $Q \times Q$ matrix, with $Q = \sum_{L=0}^{L_{max}} n_L$, is again diagonalized using standard codes. In practice the value of $L_{\max}$ is chosen to ensure a good convergence for the energies and the eigenstates of the Hamiltonian. The results given here have been obtained with $L_{\max} = N + 2$.

Note that the anisotropic rotating contribution V can in principle be included within the framework of the LLL approximation in two ways. The first approach has just been described above and consists of keeping the same Landau levels as for $A = 0$ and then diagonalizing $\hat{H}$ within the LLL. The second approach consists of calculating exactly the single-particle eigenstates in presence of the anisotropy V, and defining a new LLL accordingly [30]. The Hamiltonian is then diagonalized within this 'anisotropic' LLL. We have checked that both methods lead to very similar results for $\Omega \sim \Omega_1$. The results presented here have been obtained with the first approach.

Single particle density matrix The SPDM can be regarded as an integral operator with the kernel:

$$n^{(1)}(\vec{r}, \vec{r'}) = \langle \Psi_0 \mid \hat{\Psi}^\dagger(\vec{r})\, \hat{\Psi}(\vec{r'}) | \Psi_0 \rangle,$$

with $\hat{\Psi}(\vec{r})$ and $\hat{\Psi}^\dagger$ being the annihilation and creation field operators of an atom in $\vec{r}$. The single-particle orbitals are the eigenstates of the SPDM:

$$\int d\vec{r'} n^{(1)}(\vec{r}, \vec{r'}) \psi_k^*(\vec{r'}) = n_k \psi_k(\vec{r}).$$

If there exist a single relevant eigenvalue such that $n_1 \gg \sum_{k\geq 2} n_k$, then $\sqrt{n_1}\psi_1(\vec{r})$ has the role of the order parameter of the system. In particular, the map of the local phase of this function gives precise information on the location of vortices [15].

Adiabatic approximation The diagonalization of the many-body Hamiltonian provides the eigenstates $|\Psi_j(\Omega)\rangle$ and the eigenenergies $E_j(\Omega)$. In particular, the ground state $|\Psi_0(\Omega)\rangle$ is separated from the first excited state $|\Psi_1(\Omega)\rangle$ by an energy gap $\hbar\omega_{10}(\Omega)$, which is minimal at the avoided crossing close to Ω_1. We consider here a process where Ω is scanned linearly from $\Omega_i < \Omega_1$ to $\Omega_f > \Omega_1$ and we want to find a criterion on $\dot{\Omega}$ ensuring that the system follows adiabatically the ground state, with a negligible transition rate to the other states.

The probability for a non-adiabatic transition $\Psi_0 \to \Psi_j$ is given by [27]:

$$p_{0\to j} \leq \max \left(\frac{\alpha_{j0}}{\omega_{j0}} \right)^2$$

where $\alpha_{j0} = \langle \Psi_j | (d|\Psi_0\rangle/dt)$. We have

$$\frac{d|\Psi_0\rangle}{dt} = \dot{\Omega}\, \frac{d|\Psi_0\rangle}{d\Omega}.$$

From the eigenvalue equation $H|\Psi_0\rangle = E_0|\Psi_0\rangle$, we obtain after a derivative with respect to Ω:

$$-L_z\, |\Psi_0(\Omega)\rangle + H(\Omega)\frac{d|\Psi_0\rangle}{d\Omega} = \frac{dE_0}{d\Omega}\, |\Psi_0(\Omega)\rangle \,+\, E_0 \frac{d|\Psi_0\rangle}{d\Omega}\,.$$

We now take the scalar product with $\langle \Psi_j |$ ($j \neq 0$) and we get:

$$\langle \Psi_j | L_z | \Psi_0 \rangle = (E_j - E_0) \langle \Psi_j | \frac{d|\Psi_0\rangle}{d\Omega}\,.$$

We choose $|\Psi_j\rangle$ equal to the first excited state of the system $|\Psi_1\rangle$. The matrix element $\langle \Psi_1 | L_z | \Psi_0 \rangle$ is at most of order $N\hbar$ in the vicinity of the avoided crossing. Therefore:

$$\alpha_{10} = \langle \Psi_1 | \frac{d|\psi_0\rangle}{dt} \leq \dot{\Omega}\, \frac{N\hbar}{\hbar\omega_{10}}\,,$$

hence the condition for $p_{0\to 1} \ll 1$:

$$\dot{\Omega}\, \frac{N}{\omega_{10}^2} \ll 1\,.$$

Mean-field approach. The mean-field approach consists of assuming that all atoms are in the same state $f(\vec{r}, t) = \sum_{m=0}^{2} a_m(t)\varphi_m(\vec{r})$ with $\sum |a_m|^2 = 1$. The average angular momentum per particle is $L = |a_1|^2 + 2|a_2|^2$ and the average energy per particle $E(\psi) = \frac{1}{N}\langle f^{\otimes N} | H | f^{\otimes N} \rangle$ reads (up to an additive constant):

$$\begin{aligned} E(\psi) \;=\; & (1-\Omega)(|a_1|^2 + 2|a_2|^2) + \sqrt{2}A(a_0 a_2^* + a_0^* a_2) \\ +\; & \frac{Ng}{4\pi}\Big[|a_0|^4 + \frac{1}{2}|a_1|^4 + \frac{3}{8}|a_2|^4 \\ & + 2|a_0|^2|a_1|^2 + |a_0|^2|a_2|^2 + \frac{3}{2}|a_1|^2|a_2|^2 \\ & + \frac{1}{\sqrt{2}}(a_0 a_2 (a_1^*)^2 + a_0^* a_2^* a_1^2)\Big]\,. \end{aligned}$$

The Lagrange equations associated with this energy are $i\dot{a}_j = \partial E/\partial a_j^*$ (ref. 28), which gives for example:

$$i\dot{a}_0 = \sqrt{2}Aa_2 + \frac{Ng}{2\pi}\Big[a_0\Big(|a_0|^2 + |a_1|^2 + \frac{1}{2}|a_2|^2\Big) + \frac{1}{2\sqrt{2}} a_1^2 a_2^*\Big]$$

and two similar equations for $\dot{a}_1$ and $\dot{a}_2$. Note that in this mean-field approach, N and g have a role only through the product Ng. In particular, the fact that N is even or odd is of no relevance here.

The stationary solutions are obtained by inserting $a_m(t) = a_m(0)\ e^{-i\mu t}$ in the three Lagrange equations. A detailed analysis of the resulting 3×3 nonlinear system shows that two classes of solution exist. The first class (f_a) corresponds to $a_1 = 0$. Depending on the value of the parameters Ng, A and Ω, there may exist two, three or four solutions of this kind. After some tedious but straightforward calculation, one can obtain for this first class of solution an analytical relation between Ω and the angular momentum per particle $L = 2|a_2|^2$:

$$\Omega = 1 - \frac{Ng}{8\pi}\left(1 - \frac{3}{8}L\right) \pm \sqrt{2}\,A\frac{1-L}{\sqrt{L(2-L)}}\,.$$

The second class of solution corresponds to a non-zero value for a_1 and we have not been able to provide an exact analytical expression for the solution in this case. Using a numerical analysis, we have determined the local minima of the energy and we found that one solution of this kind exists if and only if $\Omega > 0.766$. We have compared the energy of this solution with the lowest energy of the solutions in the first class: for $\Omega < \tilde{\Omega} = 0.773$ (respectively $\Omega > \tilde{\Omega}$), the the ground state is obtained with a solution belonging to the first (respectively second) class.

The stability of the solutions of the first class ($a_1 = 0$) can be studied analytically by looking at the equation of evolution of $b_1 = a_1 e^{i\mu t}$. This equation can be linearized around $b_1 = 0$ and written in the form $i\dot{b}_1 = Ab_1 + Bb_1^*$, where the constants A and B are real numbers that can be calculated explicitly in terms of the parameters Ω, A and Ng. The stationary solution corresponds to $b_1 = 0$, and it is stable if $b_1(t)$ stays around 0 when starting from a small non-zero initial value. This happens when $|A| > |B|$, whereas b_1 undergoes an exponential divergence from any initial noise if $|A| < |B|$, signalling a dynamical instability of the solution.

[1] Weiss, P. L'hypothèse du champ moléculaire et la propriété ferromagnétique. *J. Phys.Théor. et Appliq.* **6**, 661-690 (1907).

[2] Pitaevskii, L. & Stringari, S. *Bose-Einstein Condensation*. (Oxford University Press, Oxford, 2003).

[3] Jaksch, D., Bruder, C., Cirac, J.I., Gardiner, C.W. & Zoller, P. Cold bosonic atoms in optical lattices. *Phys. Rev. Lett.* **81**, 3108-3111 (1998).

[4] Cooper, N.R. Rapidly rotating atomic gases. *Adv. Phys.* **57**, 539-616 (2008).

[5] Yoshioka, D. *The Quantum Hall Effect* (Springer, 2002).

[6] Griffin, A. *Excitations in a Bose-Condensed Liquid*, (Cambridge University Press, Cambridge, 1993).

[7] Fetter, A.L. Rotating trapped Bose-Einstein condensates. *Laser. Phys.* **18**, 1-11(2008).

[8] Feder, D. L., Clark, C.W., & Schneider, B.I. Nucleation of vortex arrays in rotating anisotropic Bose-Einstein condensates, *Phys. Rev. A* **61**, 011601(1-4) (2000).

[9] Sinha, S., & Castin, Y. Dynamic instability of a rotating Bose-Einstein condensate. *Phys. Rev. Lett.* **87**, 190402 (2001).

[10] Kasamatsu, K., Tsubota, M. & Ueda, M. Nonlinear dynamics of vortex lattice formation in a rotating Bose-Einstein condensate. *Phys. Rev. A* **67**, 033610 (2003).

[11] Butts, D.A., & Roksar, D.S. Predicted signatures of rotating Bose-Einstein condensates. *Nature* **397**, 327-329 (1999).

[12] Bertsch, G.F. & Papenbrock, T. Yrast line for weakly interacting trapped bosons, *Phys. Rev. Lett.* **83**, 5412-5414 (1999).

[13] Smith, R.A., & Wilkin, N.K. Exact eigenstates for repulsive bosons in two dimensions. *Phys. Rev. A* **62**, 061602(1-4) (2000).

[14] Jackson, A.D. & Kavoulakis,G.M. Analytical results for the interaction energy of a trapped, weakly interacting Bose-Einstien condensate. *Phys. Rev. Letters* **85**, 2854-2856 (2000).

[15] Dagnino, D., Barberán, N., Osterloh, K., Riera, A. & Lewenstein, M. Symmetry breaking in small rotating clouds of trapped ultracold Bose atoms. *Phys. Rev. A* **76**, 013625 (2007).

[16] Romanovsky, I., Yannouleas, C., & Landman, U. Symmetry-conserving vortex clusters in small rotating clouds of ultracold bosons. *Phys. Rev. A* **78**, 011606(R) (2008)

[17] Parke, M.I., Wilkin, N.K., Gunn, J.M.F. & Bourne, A. Exact vortex nucleation and cooperative tunneling in dilute BECs. *Phys. Rev. Lett.* **101**, 110401 (2008).

[18] Pitaevskii, L.P. Vortex lines in an imperfect Bose gas. *Sov. Phys. JETP* **13**, 451-454 (1961).

[19] Gross, E.P. Structure of a quantized vortex in boson systems *Nuovo Cimento* **20**, 454-477 (1961).

[20] Stringari, S. Phase Diagram of Quantized Vortices in a Trapped Bose-Einstein Condensed Gas. *Phys. Rev. Lett.* **82**, 4371-4375 (1999).

[21] Ueda, M. & Nakalima, T. Nambu-Goldstone mode in a rotating Bose-Einstein condensate. *Phys. Rev. A* **73**, 043603 (2006).

[22] Morris, A.G. & Feder, D.L. Validity of the lowest-Landau-level approximation for rotating Bose gases. *Phys. Rev. A* **60**, 033605 (2006).

[23] Wilkin, N.K. & Gunn, J.M. Condensation of Composite Bosons in a Rotating BEC. *Phys. Rev. Lett.* **84**, 6-9 (2000).

[24] Eckert, K., Schliemann, J., Bruß, D., & Lewenstein, M. Quantum correlations in systems of indistinguishable particles. *Ann. Phys. (N.Y.)* **299**, 88 (2002).

[25] Zanardi, P. Quantum entanglement in fermionic lattices, *Phys. Rev. A* **65**, 042101 (2001).

[26] Nunnenkamp, A., Rey, A.M., & Burnett, K. Cat state production with ultracold bosons in rotating ring superlattices. *Phys. Rev. A* **84**, 023622 (2008).

[27] Messiah, A. *Quantum Mechanics*, chapter XVII, §13 (Courier Dover Publications, 1999).

[28] Perez-García, V.M., Michinel, H., Cirac, J.I., Lewenstein, M. & Zoller, P. Low energy excitations of a Bose-Einstein condensate: A time-dependent variational analysis. *Phys. Rev. Lett.* **77**, 5320-5323 (1996).

[29] Garay, L.J., Anglin, J.R., Cirac, J.I. & Zoller, P. Sonic analog of gravitational black holes in Bose-Einstein condensates. *Phys. Rev. Lett.* **85**, 4643-4647 (2000).

[30] Fetter, A.L. Lowest-Landau-level description of a Bose-Einstein condensate in a rapidly rotating anisotropic trap. *Phys. Rev. A* **75**, 013620 (2007).

Acknowledgements We acknowledge discussions with I. Cirac and support of the EU SCALA and ESF Fermix Programs, Spanish MEC grants (FIS 2005-03169/04627, QOIT) and the French programs ANR and IFRAF.

Authors contributions All authors have contributed equally to this work.

Additional information Reprints and permissions information is available online at npg.nature.com/reprintsandpermissions. Correspondence

and requests for materials should be addressed to N. B.